

Optimization of PV Model using Fuzzy- Neural Network for DC-DC converter Systems

Ahmed Ali and Ali N Hasan

Department of Electrical and Electronic Engineering Science

Faculty of Engineering and Built Environment University of Johannesburg, Johannesburg, South Africa

axmedee@live.com, alin @uj.ac.za

Abstract—Due to the large demand on energy, energy sources, as well as the problems of the environment such as the dynamic weather conditions. Hence the world researchers nowadays are moving toward using solar energy because it gives different advantages over the traditional energy sources such as low maintenance costs, eternal sun energy, and the lack of revival of the gases of green houses. As a result, the photo- voltaic (PV) systems' power will be reduced. Under different weather conditions, maximizing the power point tracking (MPPT) is an important part to improve the solar systems power. In this paper, we introduce the neural network approaches for the PV systems. This paper also presents a novel application of Fuzzy Neural Network (FNN) in modeling a PV. The photovoltaic system model is designed with the use of MATLAB/SIMULINK software program with the connection of a DC-DC boost converter, a Maximum Power Point Tracking (MPPT) controller, a one-phase Voltage Source Converter (VSC) and a three-level bridge. The MPPT controller is used to cover the need for advanced controller that can detect the maximum power point in solar cell systems that have unstable current and voltage and keep the resultant power per cost low.

Keywords— Fuzzy Neural Network, maximum power point tracking, photo- voltaic.

I. INTRODUCTION

These days, solar photovoltaic (PV) us contemplated to be a common source of renewable energy because of many advantages such as the low operational costs, most maintenance free and environment friendly. Although the solar modules cost is high, the PV power generation system, in general the grids-connected types have been popularized in several countries due to their potential long-terms' benefits [1-6]. Moreover, decent financial schemes, such as the feeds-in tariff [7] as well as subsidized policy [8], all have been introduced by different countries, and that resulted in fast industry growth. PVs' Large arrays modules must be optimized in order to be fully utilized. Hence, the maximum power point tracker (MPPT) is generally employed in joint with the power converters (i.e. dc-dc converters and/or inverters). The main objective of the MPPT are to make sure if the systems can always harvest the maximum power obtained by the PV arrays. On the other hand, because of the changing of the environment conditions such as the wind changing. , the PV characteristics curve exhibit a maximum power points (MPP) that vary nonlinearly with those conditions, hence posing a challenge for the tracking algorithms. Until now,

different MPP tracking algorithms and approaches have been suggested [9]. Those approaches have different complexities, speeds and accuracy. Each approach can be classified based on the types of the control variables were used: (1) the duty cycle, (2) the current, and (3) the voltage. In the current-based and the voltage-based approaches, two methods are used. The first method is the MPP observation voltage (VMP) or/and the current IMP regarding the open circuit voltages (VOCs) [10] as well as the short circuit currents ISCs [11]. Because this method approximates constant ratios, its accuracy could not be guaranteed. As a consequence, the power will be at most below the actual MPP, which results in huge power loss [12].

The second method is to gain the PV arrays' actual operating points information (such as current and voltage). These points are updated regarding to the variations in environment conditions such as wind variations. The most common approach is the perturb and observe (P&O) approach. It depends on the voltage perturbation or the current perturbation by using available P as well as previous Pold operating power. When the P is improved, then the perturbation direction is retained; on the other hand, the perturbation direction is reversed correspondingly. Regardless of the algorithm simplicity, the P&O approach performance is with difficulty dependent on the tradeoffs between the tracking speeds as well as the oscillation that occur around the MPP [13].

II. RELATED WORKS

The small perturbation can reduce the oscillations but with speed tracking expenditure, or vice versa. Another considerable drawback of P and O is that the algorithms are very likely to lose their direction while tracking the actual MPP during the fast fluctuation of isolation. Many improvements were proposed to solve this problem- generally by taking into account the adaptive perturbation. Nevertheless, these methods are not completely adaptive as well as thus are not very efficacious [14]. Furthermore, under special conditions like module irregularities and shading, these approaches fail to track the real MPP due to the PV curves are characterized by many peaks (multiple locals and one global). Because the P&O algorithm cannot distinguish the correct peaks, its usefulness under similar condition diminish speedily [12].

Another approach is the incremental conductance (IC) that depends on cumulatively comparing the ratios of secondary of conductance with the immediate conductance [15]. Despite that IC does not experience the wasted of tracking directions. IC inherits similar problems to the P&O problems, specifically the inescapable tradeoff between the MPPT oscillation and speed. Multiple improved IC methods are suggested; for example, the researchers in [4] managed to enhance the MPP oscillations but through fast fluctuation of environment conditions, the tracking speed decreases remarkably. Furthermore, the third MPPT methods category is described by the duty cycles control. It is also known as Hill Climbing (HC), in the literature, or direct control methods. HC also operates by immediately updating the converter's duty cycles [16]. The method highly facilitates the control structures as it excludes the necessity for the proportional integral (PI) and/or hysteresis controllers. In precept, it operates on similar concepts as P&O, but instead of perturbing the current or voltage, it updates the operating points of the PV array by perturbing the duty cycle. In the absenteeism of the PI loop, the HC implementation is highly clarified and simplified. As a consequent, this approach is largely used in PV systems [17]. Nevertheless, it suffers with same disadvantages inherited by the P&O approach.

In an effort to conquer aforementioned drawbacks, many pieces of research have employed artificial intelligence (AI) methods like fuzzy logic controllers (FLC) [18] as well as neural networks (NNs) [19]. Despite that these approaches are efficacious in working with the non-linear properties of the curves of I-V, they need comprehensive computations. Because of its ability to deal with the non-linear objective functions (OF) [20], [21], EA is visualized to be very functional to handle the problem of the MPPT. Through the EA algorithms, particle swarm optimizations (PSO) are highly powerful because it's clear structure, simple implementation, as well as fast computation capabilities [22].

Referring to the [23], the diode and the current source are both in parallel form the main components of the simplest solar cell circuit. In this circuit, the output of the current source relay on the light intensity that falls on the cell. Generally, the solar cell considered as an inactive system in the dark as well as performs as a diode. On the other hand, at the light, whenever the sunshine falls down on the cell, it generates a diode current named the dark current. Nevertheless, the utilized diode influences the solar cell C-V relation. The value of both R_s and R_{sh} inside the ideal solar cell equal to zero always as a general assumption.

III. SYSTEM MODEL

The proposed system has photovoltaic generator as a main component that could be a cell, array or a module. The PV generator consists from various units, protective modules, photovoltaic cells, supports and connections. One of the essential components of the PV or the solar cells is the PN junction which is made in the thin semi-conductor layer. In the dark, the solar cell voltage and current (V-C) was defined by

[24] as an exponential relation that is very close to a diode exponential relation.

The structure of the solar system when using a DC-DC Boost converter as well as a fuzzy-neural network (FNN) control system is clear in figure 1. The input of the DC-DC is the voltage source (V_s) that generates a constant voltage output value so as to ease the energy storing within the battery. The reference voltage (V_r) considered as the best value lower than the maximum power point given from a dataset that can be figured out by employing the method of Newton. Additionally, the controller of the FNN is employed to calculate the voltage error relaying on the change rate of deliberate error as well as to control the duty cycle of the DC-DC to convert the input variable voltage to constant voltage output. Also, this controller can track the maximum power point of the PV system and save the generated energy to the battery

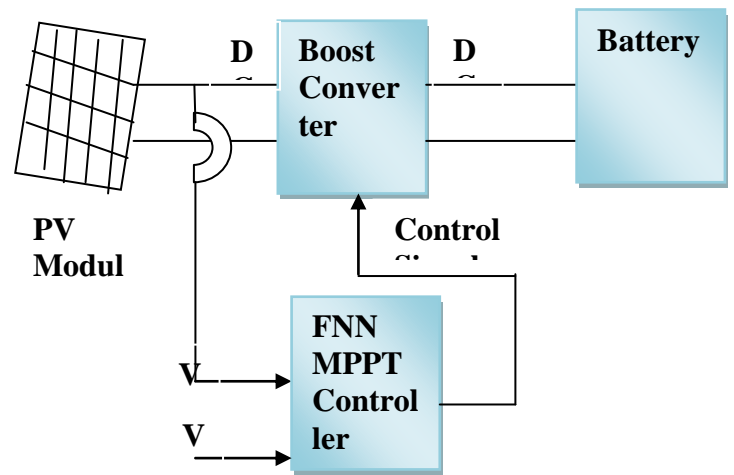


Figure 1 The structure of the solar system with a DC-DC as well as FNN control system

Table 1 factor A values relay on PV technologies.

Technology	A
Si-mono	1.2
Si-poly	1.3
a-Si:H	1.8
a-Si:H tradem	3.3
a-Si:H triple	5
Cdte	1.5
CIS	1.5
AsGa	1.3

The solar cell photo-current can be presented by:

$$I_{ph} = I_{ph(T_r)} (1 + k_i (T - T_r)) \quad (2)$$

$$I_{ph(T_r)} = S I_{sc(T_r, nom)} / S_{(nom)} \quad (3)$$

$$k_i = \frac{I_{sc(T_a)} - I_{sc(T_r)}}{T_a - T_r} \quad (4)$$

where: $I_{ph}(T_c)$ presents the PV array short circuit current, $S_{(nom)}$ presents the sun radiation level which is standard and equals to $1000W/m^2$, T_r presents the temperature which equals 25 C, $I_{sc}(T_a)$ presents the short circuit current at another reference temperature T_a , as well as k_i presents the coefficient of the short circuit temperature. After that, the reverse-saturation current which relay on the variations of the temperature can be presented as follows:

$$I_{rs} = I_{rs}(T_r) \left(\frac{T}{T_r}\right)^3 e^{\left[\frac{qV_g}{kA\left(\frac{1}{T_r} - \frac{1}{T}\right)}\right]} \quad (5)$$

$$I_{rs}(T_r) = \frac{I_{sc}(T_r)}{\left[e^{\left(\frac{qV_{oc}(T_r)}{kT_r A}\right)} - 1\right]} \quad (6)$$

$$V_{oc} = \frac{AKT}{q} \ln\left(\frac{I_{ph} - I_{rs}}{I_{rs}}\right) \quad (7)$$

where: \hat{k} presents the constant of Boltzmann, $I_{rs}(T_r)$ presents the reverse-saturation current at a standard temperature, qV_g presents the solar cell band-gap energy that is 1.115, as well as $V_{oc}(T_r)$ is the open circuit voltage at a standard temperature. Then, both the Rs as well as Rsh can be presented as following:

$$R_s = -\frac{dV}{dI_{V_{oc}}} - \frac{1}{X_v} \quad (8)$$

$$X_v = \frac{I_{rs}(T_r)q}{kT_r A e^{\left(\frac{qV_{oc}(T_r)}{kT_r A}\right)}} \quad (9)$$

$$R_{sh} = \frac{V_{oc}}{-I_{rs} \left\{ e^{\left[\frac{(qV_{oc})}{kTA}\right]} - 1 \right\}} \quad (10)$$

Through the Fuzzy Neural Network Maximum Power Point Tracking (FNN-MPPT) controller and the DC-DC converter are discussed.

A) The DC-DC Boost Converter Design

The DC-DC converts the input voltage to larger constant voltage output. DC-DC is a feed-forward system because the DC-DC only transforms controlling signals from the input to the output without any output reacts response.

The DC-DC duty cycle can be presented as following relaying on both voltages of the inductor:

$$D = \frac{V_2}{V_2 - V_1} = 1 - \frac{V_s}{V_o} \Rightarrow \frac{V_o}{V_s} = \frac{1}{1 - D} \quad (11)$$

The dynamic behavior of the boost converter can be clarified by using both KCL as well as KVL on the suggested equivalent circuit through the time of both the off as well as on. The next are the on time differential formulas:

$$V_s = L \frac{di_l}{dt} \quad (12)$$

$$0 = C \frac{dV_o}{dt} + \frac{V_o}{R} \quad (13)$$

The next are the off time differential formulas:

$$V_s = L \frac{di_l}{dt} + V_o \quad (14)$$

$$i_l = C \frac{dV_o}{dt} + \frac{V_o}{R} \quad (15)$$

The suggested four equations can be joined by employing the binary control switch (u) definition as:

$$u = \begin{cases} 1 & 0 \leq t \leq t_{on} \\ 0 & t_{on} \leq t \leq T \end{cases} \quad (16)$$

Therefore, the suggested equations will be:

$$V_s = L \frac{di_l}{dt} + (1 - u)V_o \quad (17)$$

$$(1 - u)i_l = C \frac{dV_o}{dt} + \frac{V_o}{R} \quad (18)$$

When re-ordering these equations, the dynamic equations of the converter through the period switching are:

$$\frac{di_l}{dt} = -\frac{1}{L}V_o + \frac{1}{L}V_s + \frac{1}{L}V_o u \quad (19)$$

$$\frac{dV_o}{dt} = -\frac{1}{C}i_l + \frac{1}{RC}V_o - \frac{1}{C}i_l u \quad (20)$$

The "variable structure state space model" of the converter can be presented as following. This model only has state variables.

$$\frac{d}{dt} \begin{bmatrix} i_l \\ V_o \end{bmatrix} = \begin{bmatrix} 0 & -\frac{1}{L} \\ \frac{1}{C} & -\frac{1}{RC} \end{bmatrix} \begin{bmatrix} i_l \\ V_o \end{bmatrix} + \begin{bmatrix} \frac{V_o}{L} \\ -\frac{i_l}{C} \end{bmatrix} \frac{1}{L} \begin{bmatrix} u \\ V_o \end{bmatrix} \quad (21)$$

B) Fuzzy Neural Network Maximum Power Point Tracking Controller (FNN-MPPT) Design

FNN system combines the fuzzy systems' qualities with the employ of various neural networks (NN). This FNN simplifies transforming the NN's computational power, linking configurations, as well as low level learning into high level learning and fuzzy systems that simplifies integrating the particularistic knowledge as well as analyzing fuzzy systems to NNs.

IV. SIMULATION AND NUMERICAL RESULTS

A distinctive panel must be used in experimenting and measuring the practical solar system current-voltage characteristics. The main panel parameters are illustrated in table 2. These parameters will be used in the proposed equations during the implementation of the system by using MATLAB software program. The evaluation of these characteristics will be done depending on three parameters, sun radiations, operational temperature and variables voltage as shown below.

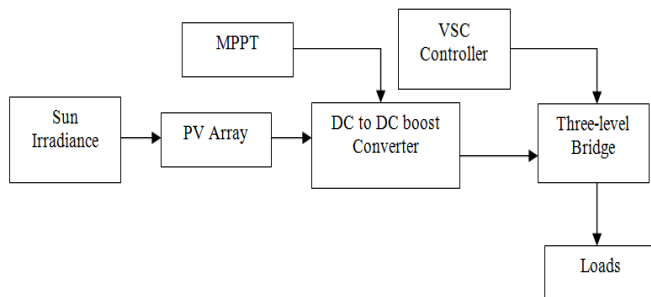


Figure 2 Overall system models

In the proposed model, a 100 kW photovoltaic array is used. This array utilizes 330 sun-power modules with a power equals to **305.2 kW** and includes 66 strings of 5 modules that are connected in series. These strings are connected in parallel. The total power equals to **66 * 5 * 305.2 = 100.7 kW**. Each module has four specifications; 96 cells that are connected in series, open circuit voltage that equals to 64.2v, short circuit current that equals to 5.96A, maximum power voltage equals to 54.7v and maximum power current equals to 5.58A.

Table 2 System Parameter

PV Module Type	KC200GH-2P
At 1000 W/m ² , 25°C	(STC)
Maximum Power	200W
Maximum Power Voltage	26.3V
Maximum Power Current	7.61A
Open Circuit Voltage (I _{oc})	32.9V
Short Circuit Current (I _{sc})	8.21A

The MPPT system uses both the incremental conductance method and the integral regulator. The MPP is achieved when $\frac{dP}{dV} = 0$, where: $P = V * I$

Thus,

$$dP = d(V * I) = I + V * \frac{dI}{dV} = 0 \quad (22)$$

$$\frac{dI}{dV} = -\frac{I}{V} \quad (23)$$

The integral regulator is used to reduce the error which is $\frac{dI}{dV} + \frac{I}{V}$. The regulator output equals to the duty cycle correction. The output voltage of the boost converter is then inserted to a three-level bridge that is shown in figure 3 below. This bridge has a snubber resistance that equals to **1x10⁶Ω**, a snubber capacitance that equals to infinity and an internal resistance that equals to **0.2x10⁻³Ω**. This bridge is controlled by a VSC control. The VSC is used in order to control the DC bus voltage at a voltage equals to 500v and maintains a unity power feature. It utilizes two control loops; an external loop that controls the DC voltage to **±250v** and internal loop that controls the grid currents. In addition, this system utilizes a sample time that equals to **100μs** for both the current and voltage controllers and for the synchronization unit. The suitable PWM waveforms resolution can be obtained from using a fast sample time that equals to **1μs** by both the boost converter and the VSC converter.

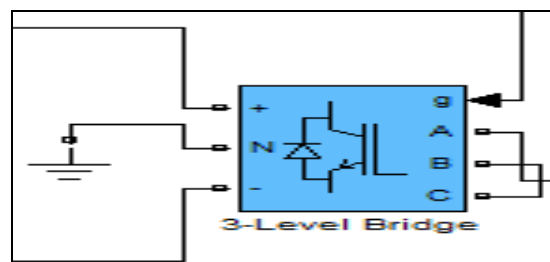


Figure 3 a three-level bridge

Figure 4 below shows the used VSC control. This control has three inputs; two voltages and one current. The output of the VSC control is multiplied by a step signal with 0.05s step time and then inserted to the three-level bridge.

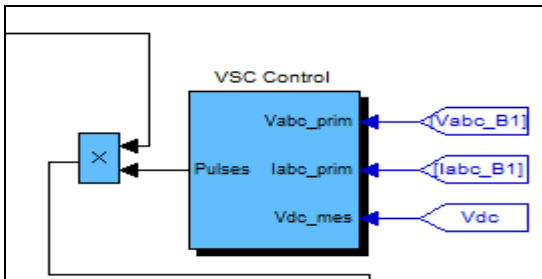


Figure 4 VSC control

A single output of the proposed three-level bridge is inserted to a circuit that contains two loads which are connected in series. The first load has a resistance that equals to $2 \times 10^{-3} \Omega$ and an inductance that equals to $250 \times 10^{-6} H$. The second load has a nominal voltage that equals to $260 V_{rms}$, nominal frequency that equals to 60Hz, active power that equals to $10^3 / 100 W$, inductive reactive power that equals to zero and capacitive reactive power that equals to 10^3 . The final output voltage of the designed photovoltaic system is shown in figure 5 below. The mean value of the resultant voltage equals to 120V.

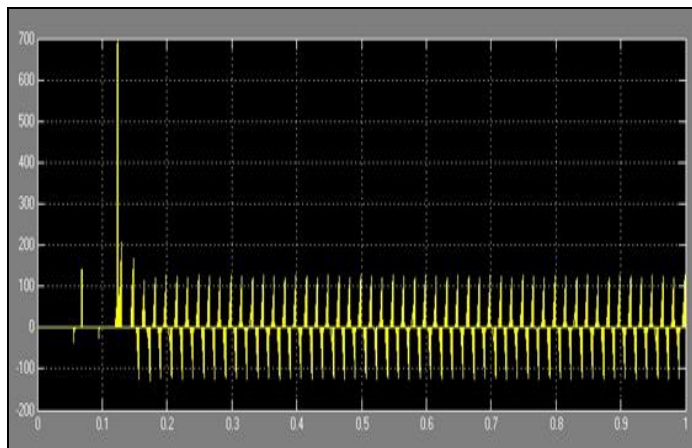


Figure 5 final output voltage

The VSC outputs are resulted from using the block that is shown in figure 6 below. In this block, the DC voltage which is the output voltage of the DC-DC buck converter is inserted to a discrete mean value that computes the mean value of the input signal over a specified basic frequency one cycle running window. The basic frequency equals to 60Hz. After that, both the reference DC voltage and the output of the discrete mean value block are inserted to a Mux that produces one output.

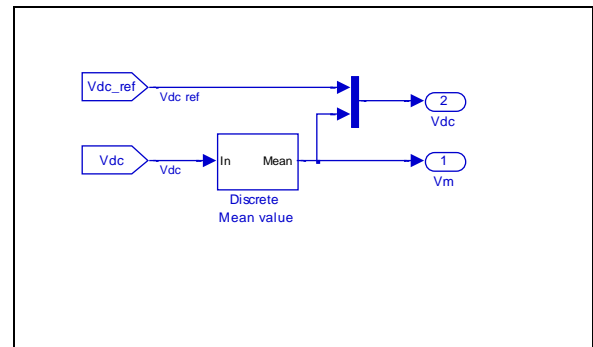


Figure 6 VSC block

Figure 7 below shows the resultant outputs of the VSC. The first figure illustrates both the reference DC voltage that has a steady value which equals to 20V and its mean value which equals to 500V. The second figure shows the modulation index that has values between zero and one.

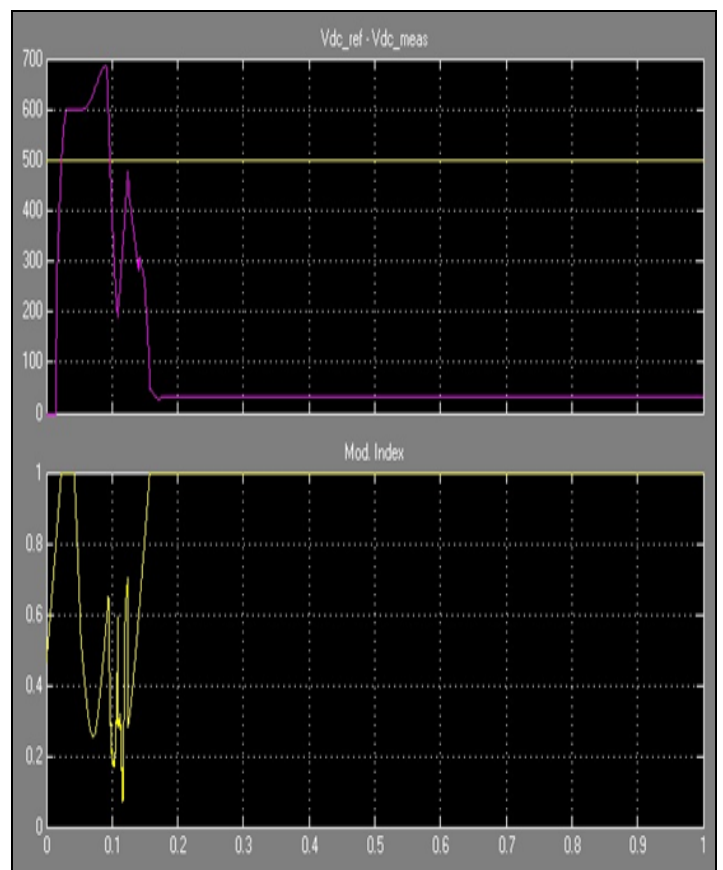


Figure 7 VSC outputs

V. CONCLUSION

Solar photovoltaic (PV) is contemplated to be a common source of renewable energy because of many advantages such as the low operational costs, most maintenance free and environment friendly. Results show that the designed PV system has a stable output voltage with a mean equals to 120V. Additionally, the mean of the DC reference voltage equals to 500V as well as the modulation index has values between zero and one. Thus, the designed PV system solves the problem of the unstable outputs of the traditional PV systems that resulted from the unstable sun radiances.

REFERENCES

- [1] L. Bangyin, D. Shanxu, and C. Tao, "Photovoltaic DC-building-modulebased BIPV system-concept and design considerations," *IEEE Trans. Power Electron.*, vol. 26, no. 5, pp. 1418–1429, May 2011
- [2] Z. Li, S. Kai, X. Yan, F. Lanlan, and G. Hongjuan, "A modular gridconnected photovoltaic generation system based on DC bus," *IEEE Trans. Power Electron.*, vol. 26, no. 2, pp. 523–531, Feb. 2011.
- [3] J. L. Agorreta, M. Borrega, Lo, x, J. pez, and L. Marroyo, "Modeling and control of N-paralleled grid-connected inverters with LCL filter coupled due to grid impedance in PV plants," *IEEE Trans. Power Electron.*, vol. 26, no. 3, pp. 770–785, Mar. 2011.
- [4] A. M. Farayola, A. N. Hasan, A. Ali, "Curve Fitting Polynomial Technique Compared to ANFIS Technique for Maximum Power Point Tracking," in 8th IEEE International Renewable Energy Congress (IREC), Amman, Jordan, 2017. .
- [5] Y. Bo, L. Wuhua, Z. Yi, and H. Xiangning, "Design and analysis of a gridconnected photovoltaic power system," *IEEE Trans. Power Electron.*, vol. 25, no. 4, pp. 992–1000, Apr. 2010.
- [6] E. Serban and H. Serban, "A control strategy for a distributed power generation microgrid application with voltage- and current-controlled source converter," *IEEE Trans. Power Electron.*, vol. 25, no. 12, pp. 2981–2992, Dec. 2010
- [7] Farayola, A. M, Hasan, A. N, and Ali, A.: Comparison of Modified Incremental Conductance and Fuzzy Logic MPPT Algorithm Using Modified CUK Converter. In: 8th IEEE International Renewable Energy Congress (IREC) 2017, Amman Jordan (2017)
- [8] L. Y. Seng, G. Lalchand, and G. M. Sow Lin, "Economic, environmental and technical analysis of building integrated photovoltaic systems in Malaysia," *Energy Policy*, vol. 36, pp. 2130–2142, 2008.
- [9] A. K. Abdelsalam, A. M. Massoud, S. Ahmed, and P. N. Enjeti, "High-performance adaptive perturb and observe MPPT technique for photovoltaic-based microgrids," *IEEE Trans. Power Electron.*, vol. 26, no. 4, pp. 1010–1021, Apr. 2011
- [10] M. A. Masoum, H. Dehbonei, and E. F. Fuchs, "Theoretical and experimental analyses of photovoltaic systems with voltage and current-based maximum power point tracking," *IEEE Power Eng. Rev.*, vol. 22, no. 8, pp. 62–62, Oct. 2002.
- [11] T. Noguchi, S. Togashi, and R. Nakamoto, "Short-current pulse-based maximum-power-point tracking method for multiple photovoltaic-andconverter module system," *IEEE Trans. Ind. Electron.*, vol. 49, no. 1, pp. 217–223, Feb. 2002.
- [12] Ahmed Ali, A., Hasan, A. N, and Marwala, T.: Perturb and Observe based on Fuzzy Logic Controller Maximum Power Point tracking (MPPT). In: IEEE International Conference on Renewable Energy Research 2014, Milwaukee, USA (2014)
- [13] S. L. Brunton, C. W. Rowley, S. R. Kulkarni, and C. Clarkson, "Maximum power point tracking for photovoltaic optimization using ripple-based extremum seeking control," *IEEE Trans. Power Electron.*, vol. 25, no. 10, pp. 2531–2540, Oct. 2010.
- [14] S. Jain and V. Agarwal, "A single-stage grid connected inverter topology for solar PV systems with maximum power point tracking," *IEEE Trans. Power Electron.*, vol. 22, no. 5, pp. 1928–1940, Sep. 2007.
- [15] K. H. Hussein, I. Muta, T. Hoshino, and M. Osakada, "Maximum photovoltaic power tracking: an algorithm for rapidly changing atmospheric conditions," *IEE Proc.-Gen., Transmiss., Dist.*, vol. 142, no. 1, pp. 59–64, Jan. 1995.
- [16] N. Femia, G. Petrone, G. Spagnuolo, and M. Vitelli, "Optimization of perturb and observe maximum power point tracking method," *IEEE Trans. Power Electron.*, vol. 20, no. 4, pp. 963–973, Jul. 2005.
- [17] A. Safari and S. Mekhilef, "Simulation and hardware implementation of incremental conductance MPPT with direct control method using cuk converter," *IEEE Trans. Ind. Electron.*, vol. 58, no. 4, pp. 1154–1161, Apr. 2011.
- [18] B. N. Alajmi, K. H. Ahmed, S. J. Finney, and B. W. Williams, "Fuzzylogic-control approach of a modified hill-climbing method for maximum power point in microgrid standalone photovoltaic system," *IEEE Trans. Power Electron.*, vol. 26, no. 4, pp. 1022–1030, Apr. 2011.
- [19] A. K. Rai, N. D. Kaushika, B. Singh, and N. Agarwal, "Simulation model of ANN based maximum power point tracking controller for solar PV system," *Solar Energy Mater. Solar Cells*, vol. 95, pp. 773–778, 2011.
- [20] K. Ishaque and Z. Salam, "An improved modeling method to determine the model parameters of photovoltaic (PV) modules using differential evolution (DE)," *Solar Energy*, vol. 85, pp. 2349–2359, 2011.
- [21] K. Ishaque, Z. Salam, H. Taheri, and A. Shamsudin, "A critical evaluation of EA computational methods for Photovoltaic cell parameter extraction based on two diode model," *Solar Energy*, vol. 85, pp. 1768–1779, 2011.
- [22] Ahmed Ali, Ilyes Boulkaibet, Bhakisipho Twala and Tshilidzi Marwala. "Hybrid optimization algorithm to the problem of distributed generation power losses. IEEE international conference on systems, man and cybernetics, 10.1109/SMC., 2016.
- [23] Ahmed Ali, Sanjeevikumar Padmanaban, Bhakisipho Twala, and Tshilidzi Marwala. "Electric Power Grids Distribution Generation System For Optimal Location and Sizing – A Case Study Investigation by Various Optimization Algorithms". *Energies Journal* 2017, 10(7), 960; doi:10.3390/en10070960